Journal of Structural Geology, Vol. 12, No. 7, pp. 851 to 867, 1990
Printed in Great Britain

0191-8141/90 $03.00+0.00

An early history of pure shear in the upper plate of the Raft River metamorphic core complex: Black Pine Mountains, southern Idaho

MICHAEL L. WELLS and RICHARD W. ALLMENDINGER

Institute for the Study of the Continents and Department of Geological Sciences, Cornell University, Ithaca, NY 14853, U.S.A.

(*Received* 5 *June* 1989; *accepted in revised form* 10 *January* 1990)

Abstract—Although commonly obscured by simple shear, pure shear fabrics occur locally within many metamorphic core complexes. The cover rocks to the Raft River metamorphic core complex exposed within the Black Pine Mountains display an early coaxial strain history which developed prior to the formation of low-angle fault-bounded allochthons. At higher structural levels this is documented by pressure shadows with straight sutures, and oppositely-rotated antitaxial calcite veins. These rocks were sub-horizontally extended parallel to bedding, by up to 160%, in an ~E–W direction. The marbles of the lowest exposed levels exhibit well-developed crystallographic preferred orientation fabrics. Calcite *c*- and *a*-axis pole figures are symmetric to slightly asymmetric, with obliquities ranging from 0° to 8°, which indicate that the percent pure shear ranges between 100 and 76%. Initial constraints on the timing of this layer-parallel extension suggest that extension was occurring locally within the Sevier belt hinterland during the late Cretaceous. These data, coupled with previous studies, suggest that pure shear might be a much more common component of strain in rocks deformed in extensional environments than is generally acknowledged.

INTRODUCTION

THE relative importance of coaxial and non-coaxial deformation during extensional deformation remains a subject of controversy as shown by work on tectonites exposed in the Cenozoic–Mesozoic metamorphic core complexes in the western United States. Generally, these *L–S* tectonites have been dramatically attenuated and, where they involve sedimentary rocks, this stretching is commonly parallel to bedding. Early studies concluded that coaxial deformation was responsible for the ductile thinning of these rock units (Compton 1980, Rehrig & Reynolds 1980, Miller *et al.* 1983). Since that time, coincident with the proliferation of sense-of-shear criteria, recognition of fabrics diagnostic of non-coaxial deformation has been widespread (Davis 1983, Lister & Snoke 1984). Nevertheless, coaxial fabrics are locally present within these tectonites (Compton 1980, Sabisky 1985, Lee *et al.* 1987), and may be of greater importance than is currently accepted. Moreover, the recognition of coaxial strain components may generally be obscured because, in a deformation involving both pure shear and simple shear components, only a minor component of simple shear strain is necessary to produce asymmetric structures (Erskine & Wenk 1987).

Middle Paleozoic strata in the Black Pine Mountains of southern Idaho, which now occur in the upper plate of the major detachment fault exposed in the Raft River metamorphic core complex, have been elongated in an E–W direction by 160% parallel to bedding. In this paper, we document the coaxial nature of this deformation, and interpret them as developing during extension. These attenuation fabrics probably formed in the late Cretaceous (Wells *et al.* 1989) and were coeval with large magnitude horizontal shortening in the foreland thrust belt ~100 km to the east. Thus, this episode of extension probably affected only the upper crust, and its continuity with mid-late Cenozoic lithospheric stretching remains unknown. Nonetheless, all subsequent events—including two phases of low-angle faulting, the first with a down-to-the-west, and the second with a down-to-the-east displacement—formed during horizontal extension of the same general orientation. Our data, and scattered examples from elsewhere in the Cordilleran hinterland (e.g. Miller *et al.* 1987), indicate that initial extension in the region of the core complexes may be older than is generally realized.

We do not dispute the importance of simple shear in extensional tectonics (e.g. Wernicke 1981). However, the data presented below clearly demonstrate that, at least in the upper plate of the Raft River metamorphic core complex, there were distinct episodes and/or distinct spatial domains in which pure shear was the dominant deformation.

GEOLOGIC SETTING

The Black Pine Mountains are located just north of the Idaho–Utah border, ~100 km to the west of the Sevier fold and thrust belt (Fig. 1). This region of northwestern Utah, southern Idaho and northeastern Nevada, has been subjected to several periods of deformation and metamorphism from Mesozoic to recent time. Rock fabrics and isotopic systems have been strongly overprinted by the most recent of these events, the Oligocene to Recent extension (Compton *et al.* 1977, DeWitt 1980, Dallmeyer *et al.* 1986, Miller *et al.* 1987),

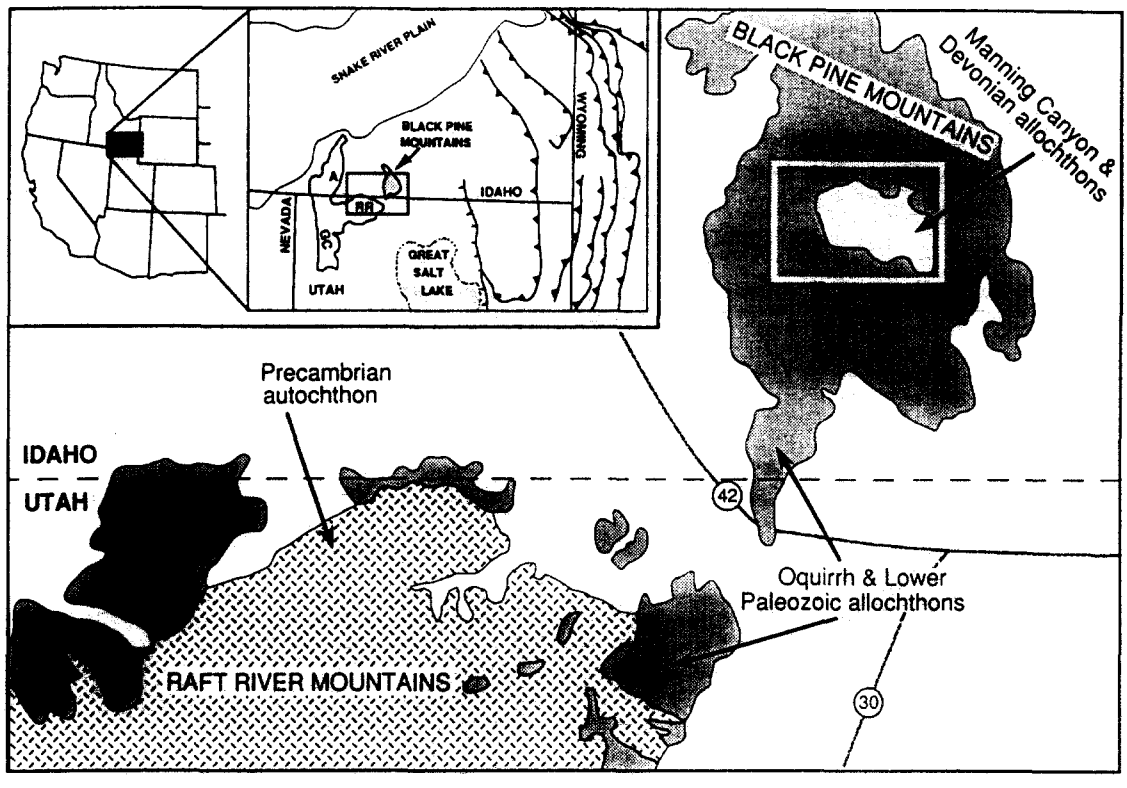

Fig. 1. Inset in top center; generalized tectonic map of the Idaho–Utah–Wyoming salient of the Sevier fold and thrust belt and its hinterland indicating the location of the Black Pine Mountains and the Raft River–Albion–Grouse Creek metamorphic core complex. Box outlined by stippled line indicates location of more detailed map showing generalized geology of the Black Pine Mountains and the eastern Raft River Mountains. In the eastern Raft River Mountains the Precambrian autochthon (shown in broken cross-hatch pattern) is separated from the Paleozoic allochthons (shown in shaded pattern) by a low-angle normal fault which dips beneath the Black Pine Mountains. Box outlined in the Black Pine Mountains indicates region shown in Fig. 2. Geology modified from Doelling (1980) and Smith (1982).

and older tectonics are not well understood. However, three regional metamorphic events appear to be discernible.

Late Jurassic–early Cretaceous metamorphism, intrusion and deformation have been documented locally (Allmendinger *et al.* 1984, Miller *et al.* 1988, Snoke & Miller 1988) although there is no consistent structural expression of this event. Structures include E-verging brittle thrust faults, ductile bedding-parallel attenuation faults, high-angle normal faults, and km-scale W-verging shear zones (Allmendinger & Jordan 1984, Miller *et al.* 1987, Miller *et al.* 1988). Many of these structures are of compressional origin, although others, commonly associated with Jurassic plutons, are extensional (Allmendinger & Jordan 1984, Miller *et al.* 1989).

Late Cretaceous metamorphism and deformation have been documented in several ranges and constitute the second phase of deformation (Allmendinger *et al.* 1984, Miller *et al.* 1987, Miller *et al.* 1988). In the northeast Nevada–northwest Utah–southern Idaho region, late Cretaceous metamorphic ages are commonly associated with younger-over-older faulting and attenuation fabrics, as well as local older-over-younger relationships (Armstrong 1976, Miller 1980, Miller *et al.* 1987). These late Cretaceous metamorphic ages probably record cooling during uplift (Snoke & Miller 1988). Farther south, however, a metamorphic event was synchronous with compressional deformation (Miller & Gans 1989). These structures are generally coeval with peak shortening in the foreland fold and thrust belt farther east.

Thirdly, regional Tertiary extensional deformation, local metamorphism and intrusion have produced structures ranging from brittle normal faults in unmetamorphosed rocks to folds and ductile shear zones in metamorphic rocks. The Tertiary deformation produced the detachment faults and many of the mylonitic zones exposed in the core complexes of this region (Compton *et al.* 1977, Malavieille 1987).

STRUCTURE

The Black Pine Mountains lie 10 km to the northeast of a large, highly-extended terrane exposed within the Raft River, Grouse Creek and Albion mountains (Fig. 1). This extended terrane shares many attributes with the family of structural associations termed "metamorphic core complexes" (Crittenden *et al.* 1980). The Raft River Mountain metamorphic core and the Black Pine Mountains are separated by a major down-to-the-east, low-angle normal fault that is exposed within the Raft River Mountains and dips ENE beneath the Black Pine Mountains. The presence of the low-angle fault in the valley separating the two ranges is confirmed by seismic reflection (Covington 1983) and borehole data (Oriel *et al.* 1978, Smith 1982).

In the southern Black Pine Mountains, five structural plates are separated by low-angle faults that place younger rocks over older rocks (Smith 1982, 1983) (Fig. 2). These include, from the base upwards: the Devonian Guilmette Formation (Dg), the Lower Mississippian and Upper Pennsylvanian Manning Canyon Shale (PMmc), and three plates composed of Pennsylvanian to Permian Oquirrh Group rocks: the Oquirrh limestone plate (Pol), the Oquirrh dolomite plate (Pold), and the Oquirrh sandstone plate (Pos, Fig. 2). The Guilmette Formation is the structurally lowest allochthon and its basal contact is not exposed. The strain analysis described in this paper will be restricted to the Devonian Guilmette Formation and the Pennsylvanian Oquirrh Group carbonates.

Five metamorphic and/or deformational events are

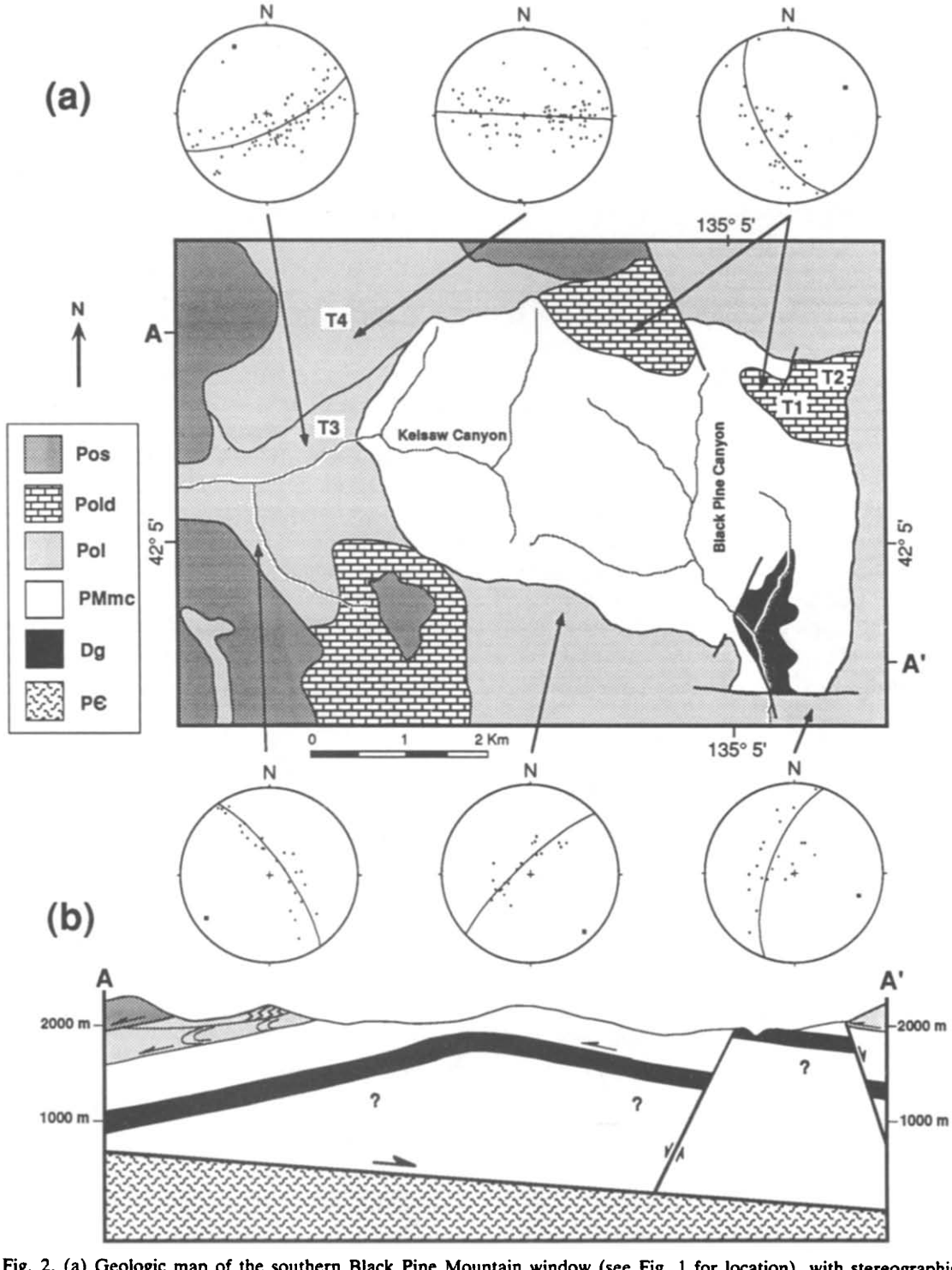

Fig. 2. (a) Geologic map of the southern Black Pine Mountain window (see Fig. 1 for location), with stereographic projections of poles to bedding for various structural domains. All contacts shown are faults, thin lines indicate low-angle faults sub-parallel to bedding, thicker lines indicate high-angle normal faults. Locations T1, T2, T3 and T4 are discussed in section on strain path. Pos, Pennsylvanian–Permian Oquirrh sandstone; Pold, Pennsylvanian Oquirrh dolomite; Pol, Pennsylvanian Oquirrh limestone; PMmc, Mississippian–Pennsylvanian Manning Canyon shale; Dg, Devonian Guilmette limestone; P€, Precambrian parautochthon. (b) Geologic cross-section of the southern Black Pine window.

recorded in the Black Pine Mountains (Wells & Allmendinger 1987, Wells 1988, Wells *et al.* 1989). From oldest to youngest these include: (1) static metamorphism (M_1) to 350–400°C recorded by pre-tectonic chloritoid porphyroblasts in the Manning Canyon Shale and conodont color alteration indices of 5–5.5, possibly synchronous with emplacement of late Jurassic sills; (2) E–W layer-parallel elongation of 160% associated with synkinematic metamorphism (M_2) and growth of white mica along cleavage; (3) generally W-vergent low-angle faulting and overturned to recumbent folding; and, although their relative sequence is not known; (4) and (5) doming and high-angle normal faulting.

The strained features within the Oquirrh, which document pure shear and are the focus of this paper, formed early in this structural history (see 2 above) and prior to the displacement of allochthons in simple shear. This is clearly shown by the much greater coherence of the fabrics of episode 2 after the effects of folding during episode 3 are removed (Fig. 3). Those folds formed synchronously with, or are truncated by, the first of two phases of low-angle faulting, which had a top-to-the-west sense-of-shear. Episodes 4 and 5 are thought to be related to the second low-angle faulting event: down-to-the-east movement on the Raft River detachment during the middle Miocene.

The age of layer-parallel elongation is constrained by isotopic analyses from the Manning Canyon Shale. Smith (1982) reported nine K–Ar whole rock analyses, seven of which yielded apparent ages between 93 and 111 Ma. Our preliminary $^{40}Ar/^{23}Ar$ whole-rock analyses of this slate (total gas age 93 ± 5.9 Ma, Wells *et al.* 1989) indicates that the apparent ages reported by Smith (1983) record a late Cretaceous metamorphic event rather than partial resetting of detrital ages during a Cenozoic thermal event. This metamorphic event is interpreted to represent the age of deformation associated with synkinematic growth of fine-grained white mica (M_2). This paper will focus on the probable late Cretaceous layer-parallel elongational fabrics, which are of particular consequence because they apparently developed during progressive pure shear. A description of the strain and strain orientations within the Pennsylvanian and Devonian carbonates will be followed by documentation of the magnitudes of finite strain. These data will then be incorporated with incremental strain indicators to document the coaxiality of the strain path for these fabrics recording bedding-parallel elongation.

STRAIN IN OQUIRRH GROUP CARBONATES

Description

Oquirrh Group carbonates are the dominant lithology in the southern Black Pine Mountains, and contain the greatest diversity of minor structures, including: (1) cleavage; (2) folded veins; (3) boudinaged veins; (4) deformed fossils; (5) pressure shadows; and (6) weak to moderate stretching lineation. Single features that provide a complete description of the three-dimensional finite strain were generally not widely distributed, therefore the kinematic analysis was synthesized from several qualitative and quantitative strain indicators over a large area. In describing principal axes of the finite-strain ellipsoid, the maximum, intermediate and minimum principal-stress axes will be referred to as X, Y and Z axes, respectively. Because folding occurred after the formation of the strained features, all measurements were unfolded about their respective fold axes and will be discussed in their unfolded orientations (e.g. Fig. 3).

The Oquirrh Groups exhibits two cleavages. The earliest is a ubiquitous near-bedding-parallel cleavage that pre-dates folding. The second is an axial-planar pressure-solution cleavage that is very well developed in the hinge regions of folds. At outcrop-scale, the earlier cleavage ranges from a spaced pressure-solution cleavage to a more continuous crystal-plastic foliation.

At least three generations of veins occur within the Oquirrh Group rocks (Fig. 4). The first two have been micro-folded or boudinaged depending on their orientation relative to cleavage. Early, pre-metamorphic black calcite veins oriented at low-angles to cleavage record the largest amount of elongation. Second generation white calcite fills the black calcite boudin necks and also forms veins that have, themselves, developed pinch-and-swell structure. Quartz veins are the third generation, infilling incipient necks in second generation white calcite veins and forming veins that cross-cut both first and second generation veins. Veins that were oriented at moderate to high angles to cleavage have been folded and record shortening perpendicular to cleavage. Where segments of folded veins have rotated

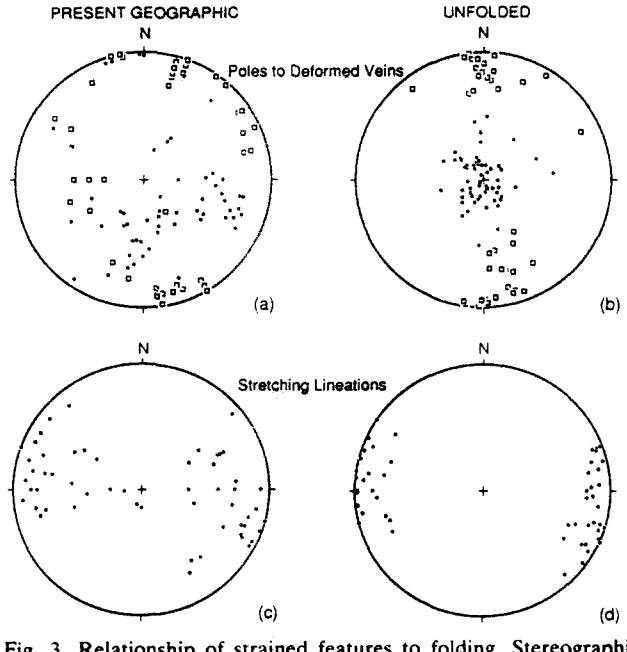

Fig. 3. Relationship of strained features to folding. Stereographic projection of: (a) poles to deformed veins in their present orientation; (b) unfolded poles to deformed veins (circles = poles to boudinaged veins, boxes = poles to folded veins); (c) stretching lineations in their present orientation; (d) unfolded stretching lineations. The more consistent orientation of unfolded features illustrates that these strained features developed prior to folding.

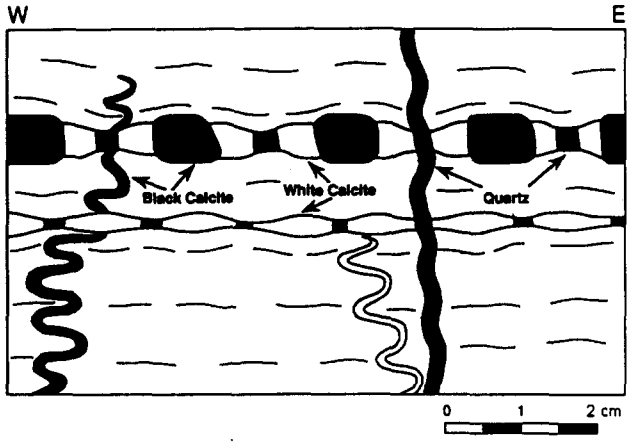

Fig. 4. Sketch of the three generations of veins. Dark shaded pattern represents early pre-metamorphic black calcite veins which record the greatest amount of strain. White calcite (unshaded) is the second generation vein material, and quartz veins (horizontal ruled pattern) develop last. Boudinage and pinch-and-swell are predominantly symmetric.

into the field of elongation during buckling, boudinage has developed.

Orientation of finite-strain axes

The orientation of the finite-strain axes can be deduced from analysis of the deformed veins. The following measurements were made on folded and boudinaged veins in the field: (1) plane of vein; (2) exposure plane; (3) amount of two-dimensional vein shortening or elongation; and (4) fold axis and boudin neckline orientation.

The direction of vein elongation and shortening (principal axes for the strain ellipse within the plane of the vein) were determined by taking the normal to the boudin neckline or fold axis, respectively, within the plane of the vein. Vein elongation (Fig. 5a) and shortening directions (Fig. 5b) yield distinct bulls-eye patterns representing extension and shortening axes, respectively. An extension axis of approximately 085° and a shortening axis near vertical are indicated. Poles to boudinaged veins also indicate a near vertical shortening axis (Fig. 5c). During deformation, veins undergoing elongation will tend to rotate towards parallelism with the XY plane of the finite-strain ellipsoid. Thus, poles to extended veins after deformation will cluster about the pole to the XY plane and define the shortening axis.

Axes of boudin necklines cluster in the N–S, near-horizontal orientation (Fig. 5d). Previous work (Sanderson 1974, Burg & Harris 1982) has shown that boudin necklines may have several possible orientations with respect to the strain ellipsoid; they may be: (1) oriented randomly to systematically within a plane as in the case of uniaxial flattening; (2) clustered parallel to the Y axis; or (3) oriented 45° from the Y axis within the plane of maximum shear. By comparison with other data (i.e. near-vertical shortening as indicated by sub-horizontal cleavage and the orientation of vein shortening axes, and near E–W elongation shown by stretching lineations—(to be discussed below), we suggest that the intermediate axis of the finite-strain ellipsoid (Y axis) is oriented in a subhorizontal, N–S position. Therefore the boudin necklines in the Black Pine Mountains are interpreted to lie in the Y direction.

Folded-vein hingelines, on the other hand, are more difficult to interpret. The majority of the axes are oriented approximately E–W and a smaller population from more highly-shortened veins are oriented N–S (Fig. 5e). However, this is in part an effect of the original orientation of the veins; the majority of the veins are presently E–W-striking, with a minor population of veins with N–S strikes. Fold axes parallel to both Y and X are explained by the observation that, when one principal direction within a vein is in the direction of shortening, the other principal direction is a potential fold axis. Furthermore, when planes are oriented such that there are both contractional and elongational longitudinal strains within the plane, fold axes will develop parallel to the extensional axis (Flinn 1962). In the case of the E–W-striking veins, fold axes developed parallel to the X axis, whereas the more highly deformed, N–S-striking veins have axes parallel to Y. Therefore, the orientations of the vein fold axes are strongly influenced by the original orientations of the veins. Fold axes are oriented perpendicular to the shortening direction, cluster about the apparent extension axes within the two vein planes, and are close to the Y and X finite-strain ellipsoid axes.

Deformed crinoids and brachiopods are present locally within the Oquirrh limestones. Crinoids have been extended and infilled with calcite, deformed by pressure solution, or flattened by crystal-plastic mechanisms. Pressure shadows are developed locally around semi-rigid to rigid clasts (pyrite, chert, fossils). These shadows contain fibrous quartz and calcite and will be discussed in more detail below.

A variety of linear features, including syntectonic mineral fibers, elongate clasts, pulled-apart clasts and fossils, and mineral streaking occur within the strained limestones of the Oquirrh Group. Although these lineations are only developed locally, they are generally consistent in orientation (Fig. 5f). Because some of the lineations are defined by syntectonic mineral fibers which grew in the principal extension direction, and because of the similarity in orientation of all lineations, they are interpreted as stretching lineations parallel to the X axis of the finite-strain ellipsoid. Contouring of these lineations after unfolding yields an average orientation of approximately 095° (Fig. 5f). All of these data on strain axis orientation consistently yield the following orientations for the principal finite strains: X axis, E–W and subhorizontal; Y axis, N–S and subhorizontal; Z axis, subvertical.

Magnitudes of principal finite strains

Measurements of fibrous pressure shadows indicate the direction and amount of incremental extensions (Ramsay & Huber 1983). In the Black Pine Mountains, pressure shadows are developed locally around pyrite,

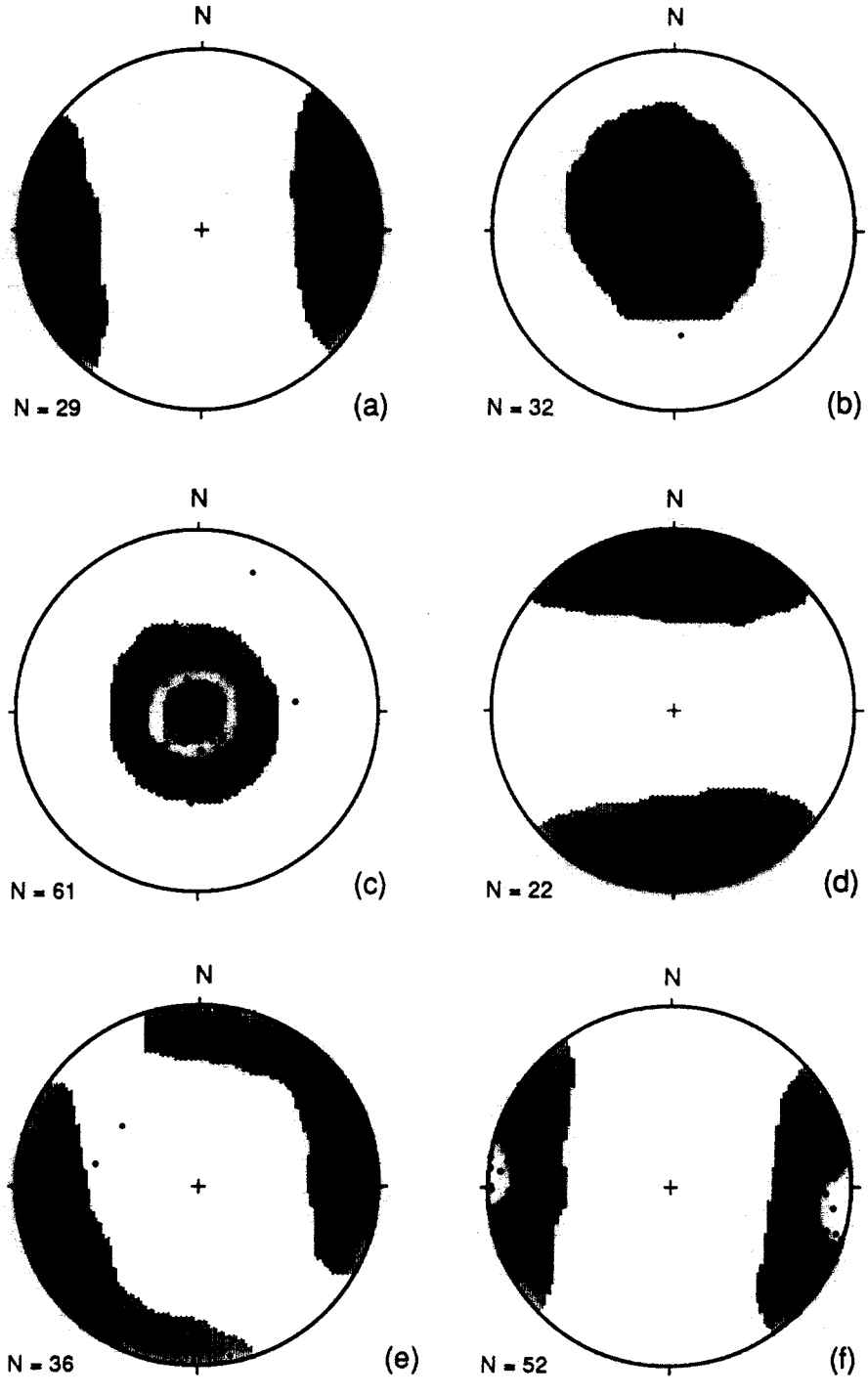

Fig. 5. Contour diagrams of unfolded structural features yielding orientations of finite-strain axes. Contouring is by the Kamb method; contours of 3, 6, 9, 12 and 15 sigma. (a) Directions of vein extension from boudinaged veins; (b) directions of vein shortening from folded veins; (c) poles to boudinaged veins; (d) vein boudin necklines; (e) vein fold hingelines; (f) stretching lineations.

crinoid platelets and detrital grains. Elongation measurements were determined from quartz pressure shadows around pyrite within a siltite interbed in Oquirrh dolomite (Pold, T1, Fig. 2), following the methods of Ramsay & Huber (1983). Measurements were made in the *XZ* plane (parallel to lineation and perpendicular to cleavage). These data show moderate scatter, but are of the order of 160% or greater in the *X* direction (Fig. 6a). From this same locality, another strain indicator suggests a similar value of elongation: rotated syntectonic veins with up to 45° of fiber curvature (described in detail under section on strain path) require a minimum of 145% elongation to account for their degree of rotation (Fig. 6b).

This value of elongation is also compatible with other scattered elongation measurements from the Oquirrh limestone (Pol). At one locality, pulled apart crinoid ossicles record elongation values from 60 to 190%. Pressure shadows from chert-rich horizons (T4, Fig. 2) within the Oquirrh yield variable elongation values from 80 to 175%. However, generally the pressure shadows from lithologies other than at T1 were contained within a

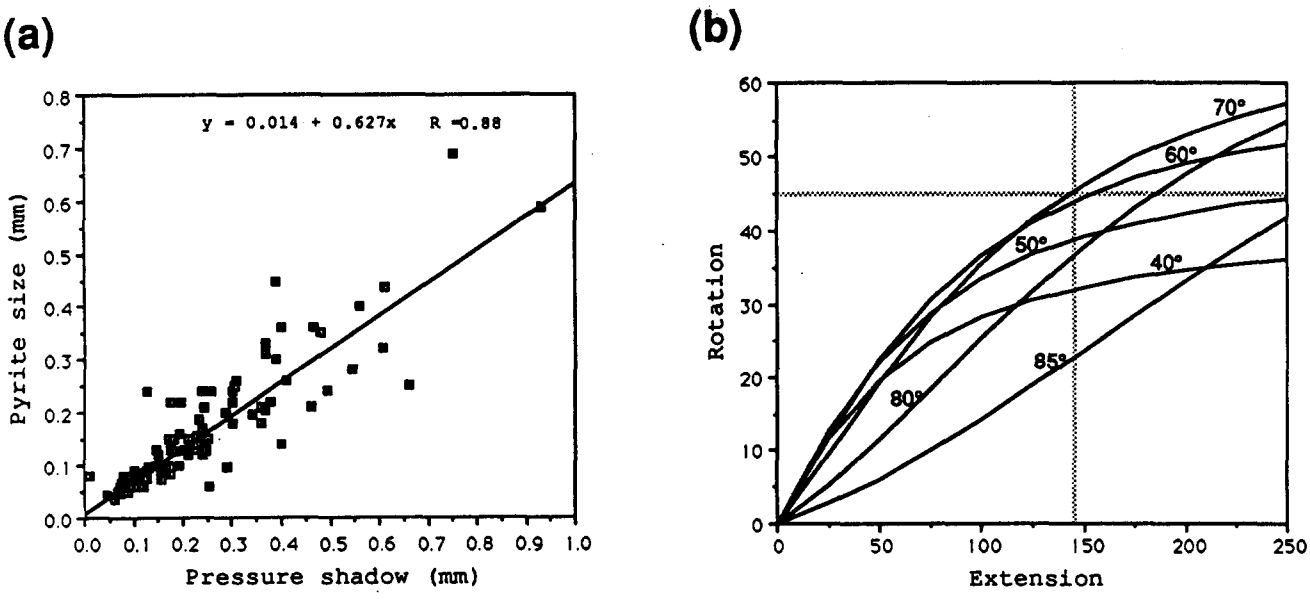

Fig. 6. Strain measurements from locality T1. (a) Extension measured from pressure shadows. Graph of length of pressure shadow vs pyrite size for 104 measurements. The least-squares best-fit to the data yields 160% extension ($\frac{1}{0.627}$). (b) Extension determined from the amount of rotation of syntectonic veins. Graph illustrates the amount of extension indicated by the amount of vein rotation for veins of various initial orientations. Numbers on curves are vein inclinations relative to cleavage. Minimum extension for a 45° rotation is 145%.

more coarse grained and less homogeneous matrix, and pressure shadow-related strain is very heterogeneous.

Minimum values of shortening and elongation have also been determined by measuring the present length of shortened lines and extended lines (folded veins and boudinaged veins) and the reconstructed original length of these lines (Fig. 7). The measurement of deformed veins for this area proved to be only a rough guide to the minimum strain magnitudes. The pressure shadows apparently were better recorders of the bulk strain than the deformed veins because: (1) the grains about which the pressure shadows formed were present throughout the entire deformation, whereas the veins probably formed during the deformation; (2) elongation values from boudin reconstructions provide only a minimum value of bulk elongation because many boudinaged veins exhibit ductile thinning and necking, and because there were several periods of veining; and (3) at single outcrops, veins of the same apparent generation and of similar orientations record different amounts of measurable deformation. The strain magnitude data, taken as a whole, indicate that horizontal elongation was locally as great as 160%.

Several observations suggest that the strain in the Oquirrh approaches plane strain. At localities with pressure shadows, no appreciable elongation was noted

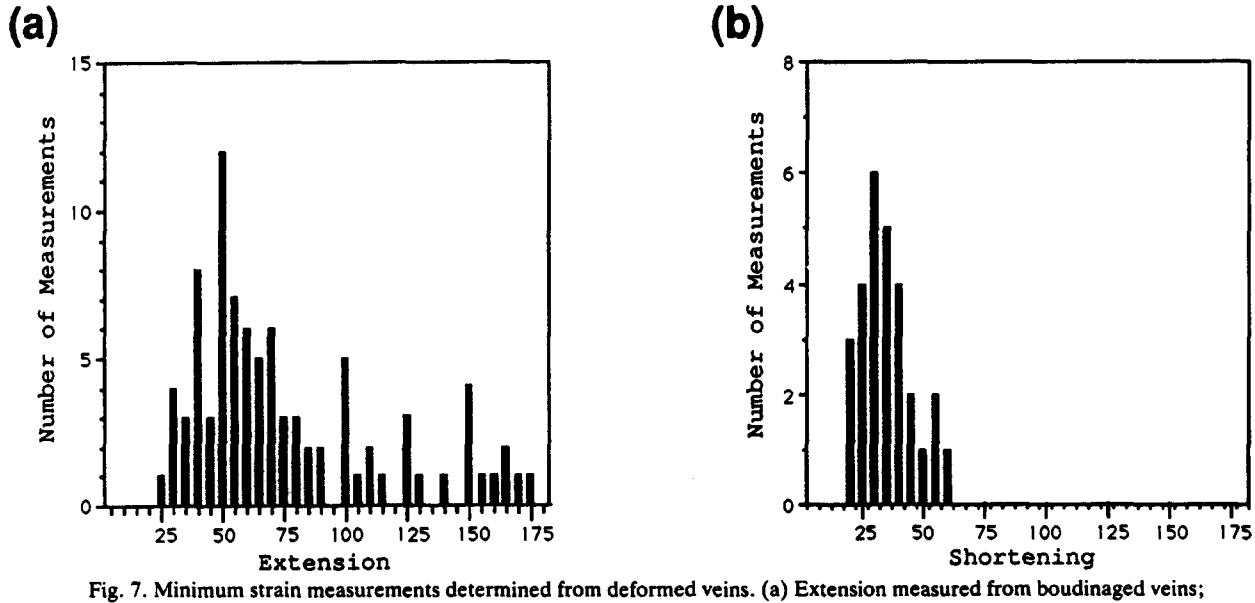

Fig. 7. Minimum strain measurements determined from deformed veins. (a) Extension measured from boudinaged veins; (b) shortening measured from folded veins. Data are combined from all localities within the study area, and illustrate the large variation in strain recorded by veins. Note that there were three generations of veining, and these measurements are not differentiated according to vein generation.

parallel to Y, although local elongations of 15% were measured. The deformed veins also provide constraints. Sanderson (1974) examined the orientations of stretching lineations and boudin axes for the five types of strain ellipsoids (after Ramberg 1959, and Flinn 1962); types 1–5 correspond to $k = 0$, $k = 0.22$, $k = 1$, $k = 7.5$ and $k =$ infinity (where $k = ((S_1S_2) - 1)/((S_2/S_3) - 1)$ and S_1, S_2 and S_3 refer to the principal stretches). By comparing the Black Pine data with the theoretical patterns developed by Sanderson (1974, figs. 2 and 3), types 1 and 2 strain ellipsoids (oblate spheroids) can be ruled out because neither stretching lineations parallel to Y (N–S-trending stretching lineations) nor boudin necklines parallel to X (E–W-trending boudin necklines) are present in the Black Pine data. For $k \geq 1$, boudinage is restricted to planes that pass through the field of finite elongation and in all cases boudin necklines are parallel to Y; this is the case with the Black Pine data. Taken together, the deformed vein data indicate that a flattening-type deformation can be ruled out, and although more speculative, the negligible to minor elongation (recorded in pressure shadows) parallel to Y suggests that conditions, rather than being constrictional, were close to plane strain.

Strain path

A notable observation from examination of the ductile fabrics of these rocks is the virtual absence of features suggestive of simple shear. If as much as 160% elongation was produced during simple shear, the angle between shear planes and the foliation would be approximately 21°. However, in the Oquirrh, there is no secondary fabric of this or any other orientation in the array of features which formed prior to folding. The cleavage–foliation fabric is thought to represent a flattening foliation (S-surface) and not a shear foliation (C-surface) for several reasons: no offset markers were noted across this fabric, shortening strains are normal to these surfaces (pressure solution, folded veins), and elongational strains occurred within the plane of these surfaces (pressure shadows and overgrowths, boudinaged veins).

Asymmetric boudinage has been shown to develop in regions of high shear strain (Hanmer 1986, Gaudemer & Tapponnier 1987, Goldstein 1988). The development of boudinage and pinch and swell structure in the Black Pine Mountains, however, is predominantly symmetric (Fig. 4). The presence of symmetric pinch and swell structure is especially striking, because this structure, if developed in a zone of simple shear, would be expected to exhibit a geometry reminiscent of the stair-step geometry seen in type II S–C mylonites (Lister & Snoke 1984). Asymmetric, en échelon boudins were noted, but they were both very scarce and not consistent in sense of asymmetry. Rather than resulting from simple shear, these rare en échelon boudins are interpreted to form during rotation of extending veins in pure shear (see Ramsay & Huber 1983, p. 99).

Despite the abundance of small-scale structures, no features indicative of non-coaxial deformation were developed. This in itself is suggestive that the fabrics were developed during progressive pure shear rather than simple shear. This conclusion is further substantiated by detailed observations from four outcrops where a coaxial incremental strain history can be determined. These localities are currently located in two different structural plates, and two localities are in Black Pine Canyon and two are in Kelsaw Canyon (Fig. 2). Although these features are not widespread, the strain path determined for these localities probably is relevant to the southern Black Pine Mountains. Locality T1 from the Oquirrh dolomite (Pold) (Fig. 2) will be described below.

A 1 ft thick siltite bed within the Oquirrh limestone is cut by many syntectonic calcite veins that are restricted to this horizon. Cleavage is well-developed and subparallel to the lithologic contact. On cleavage surfaces, a faint stretching lineation is present and the vein–cleavage intersections are approximately normal to this lineation. These veins are antitaxial and composed of fibrous calcite; the fibers exhibit curvature of up to 45° (Fig. 9a). The veins themselves are slightly folded, and lie in the shortening fields for both incremental and finite shortening. Veins of opposite inclination with respect to the cleavage normal show the opposite sense of sigmoidal fiber curvature. The vein fibers themselves display e-lamellae and weak undulatory extinction indicating that they underwent plastic deformation. However, the parallelism between the last increment of fiber growth (at the vein wall), cleavage and the elongation direction as indicated by pressure-shadow growth in the surrounding matrix (described further below) indicates that the fiber curvatures are not due to deformation, but rather simultaneous vein rotation and fiber growth.

Mineral fibers in syntectonic veins have been shown to grow parallel to the incremental elongation direction, as is the case with displacement controlled, fibrous pressure shadows (Durney & Ramsay 1973, Ramsay & Huber 1983). The curved fibers within individual veins record rotation of either (1) material lines through incremental-extension axes or (2) external rotation. A progressive coaxial deformation is the simplest explanation for the opposing senses of curvature in veins which are oriented with opposite inclinations to the cleavage normal. Veins initially oriented at slightly opposing inclinations to the shortening direction experience rigid-body rotation of the opposite sense and record progressive rotation in their synkinematic mineral-fiber growths. Locally T2 also exhibits this same type of fibrous antitaxial vein structure.

Figure 8 illustrates the inferred, sequential opening of these syntectonic veins, beginning with tension fracturing and fibrous-calcite infilling followed by progressive vein rotation, vein opening and infilling. This pure shear stretching was oriented approximately E–W as indicated by unfolded mineral lineations within the Oquirrh Group (Fig. 5f).

As a further check on the pure shear interpretation,

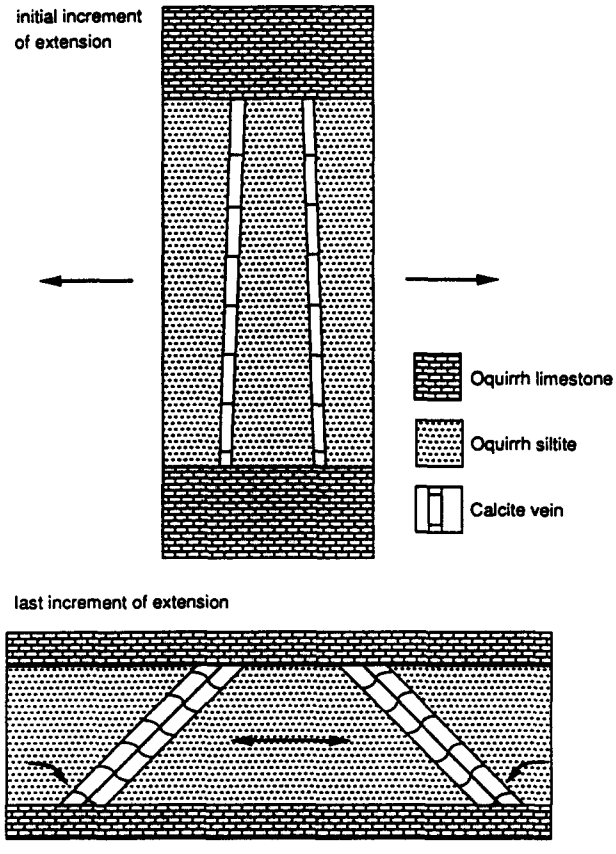

Fig. 8. Initial and final stages in a progressive coaxial deformation path as illustrated by the development of curved-fiber antitaxial calcite veins at localities T1 and T2. Diagram is scaled for 160% extension.

the pre-deformational orientation of the veins was reconstructed. If the veins opened and rotated during the same progressive coaxial deformation, then they should originally have been at a high angle to the present cleavage. However, if produced by simple shear they would be inclined all in the same direction and at a moderate angle to the cleavage normal. To check the compatibility of the observed and predicted geometries, nine veins have been restored to their pre-rotational position by back-rotating the veins by the amount of curvature recorded in the fibers, about an axis defined by the pole to the plane containing fiber orientations. The restored veins are all of a fairly similar steep orientation, with an average dip of 81°, and not all are inclined in the same direction with respect to the cleavage normal.

Within the siltite surrounding the veins, fibrous-quartz pressure shadows occur around pyrite grains. These pressure shadows are face-controlled, and the displacement direction is marked by the suture between fiber growths originating from crystal faces of differing orientation (Durney & Ramsay 1973, Ramsay & Huber 1983). The majority of the sutures are straight (Figs. 9b & c). Curved fibers and sutures with curvatures up to 20° were noted but the fiber curvatures were not systematic; approximately equal numbers suggested clockwise rotation as anticlockwise rotation. In addition, these curved, face-controlled fibers exhibited undulatory extinction. Together, this suggests that the fiber curvature was due to deformation, not synchronous rotation and growth. Therefore, these pressure shadows as a whole are interpreted to be the result of coaxial deformation.

A microscopic-scale example of oppositely rotated syntectonic veins is present at locality T3 (Fig. 2). Syntaxial quartz veins or extensional fillings are present within limestone. In thin section, veins of opposite inclination relative to the cleavage normal exhibit the opposite sense of fiber curvature (Figs. 9d & e). Veins oriented perpendicular to cleavage have straight fibers, indicating that veins of this orientation did not rotate during deformation and fiber growth. By arguments similar to those presented above for localities T1 and T2, this microstructure documents a pure shear deformational path.

The final locality where a coaxial history is illustrated is situated on the north side of Kelsaw Canyon (T4, Fig. 2). An impure limestone exhibits a strong lineation defined by elongate and pulled apart detrital chert clasts. Fibrous quartz infills the pulled apart chert (Fig. 9f). In thin sections cut parallel to the lineation and perpendicular to foliation, the foliation trace is parallel to the fiber orientation. These fibers are displacement controlled and are generally straight, indicating coaxial deformation. Furthermore, tensional fractures or incipient pull-aparts (which form parallel to the principal compressive stress) are oriented perpendicular to the foliation and fibers, indicating coaxiality between incremental and finite strains.

The above observations from localities T1 to T4 lead us to interpret the >150% bedding-parallel elongation within the Oquirrh Group, which developed prior to folding, as having developed during progressive pure shear deformation.

STRAIN IN DEVONIAN GUILMETTE

The lowest stratigraphic and structural unit exposed, the Guilmette Formation, displays the best developed tectonite fabrics of any carbonate units within the Black Pine Mountains. Two hundred meters of highly foliated and lineated marble are exposed in Black Pine Canyon (Fig. 2). This unit was studied to determine the strain history for this structural level, and to allow comparison to structurally higher Oquirrh carbonates.

The Guilmette marbles exhibit a generally bedding-parallel foliation that is defined by elongate calcite grains (Fig. 10a) and mm- to cm-scale compositional layering. The microscopic foliation is generally parallel to the compositional foliation, except where the latter has been folded. The lineation present on foliation surfaces reflects the shape fabric of calcite. This lineation trends ~098° and is interpreted to represent a stretching lineation (Fig. 10b). Aspect ratios of calcite grains (measured parallel to lineation and perpendicular to foliation) average 2.5, and grain long-axis dimensions average 0.6 mm.

The age of this grain shape fabric is undetermined, however several observations suggest that this Guilmette fabric is related to the pure shear fabrics recorded

within the Oquirrh Group carbonates: (1) stretching lineations in the Guilmette (average ~098°) are very similar in orientation to the extension direction determined from the higher Oquirrh Group carbonates (Figs. 5c & f); (2) both the Oquirrh Group carbonates and the Guilmette marbles have a similar structural sequence with W-verging simple shear occurring after the development of these layer-parallel elongational fabrics; and (3) as will be discussed below, the strain path responsible for the fabric development in the Guilmette is similar to the strain path for the Oquirrh Group—predominantly pure shear.

As mentioned above, simple shear fabrics are locally present within the Guilmette marbles, and appear to post-date the dominant foliation development. Locally in more argillaceous horizons, a weak secondary cleavage dipping NE is superimposed on the dominant foliation and mm- to m-scale shear zones are locally present throughout the exposed section. These shear zones are parallel to bedding and the dominant foliation. Macroscopic as well as microscopic sense-of-shear criteria consistently yield tops-to-the-west-southwest shear. The former include foliation–shear-zone boundary relationships, whereas the latter include asymmetric porphyroclasts, and *S–C* relationships with shear bands. These shear bands exploit pre-existing grain boundaries and twin lamellae, and a gradual progression in shear band development is present within thin section, grading from elongate grain shape fabrics with sharp grain boundaries, to incipient recrystallization along grain and twin boundaries, with progressive widening of the zones of recrystallization until shear bands are developed. These shear zones and bands are interpreted to relate to a younger deformation and will not be discussed further here. The flattening fabric defined by the elongate grains upon which the shear zones are superimposed is the focus of this section. Mesoscopic features useful in strain analysis are very scarce, so the strain in this rock was investigated using techniques of lattice preferred orientation analysis of calcite in marbles.

A large body of work has documented the development of preferred orientation fabrics in calcite-bearing rocks. Early studies of coaxial deformation of limestones have documented the expected orientations of crystallographic features such as *c*-axes, *a*-axes and *e*-lamellae (Turner & Ch'ih 1951, Turner *et al.* 1956, Turner & Weiss 1963). More recent experimental studies (aided by X-ray diffraction pole figure texture analysis) and computer simulations of pure shear (Casey *et al.* 1978, Wagner *et al.* 1982, Wenk *et al.* 1987) have extended our knowledge of preferred orientation development during coaxial deformation. The expected fabric development during *non-coaxial* deformation has recently been determined both experimentally and theoretically (Rutter & Rusbridge 1977, Kern & Wenk 1983, Schmid *et al.* 1987, Wenk *et al.* 1987), and strain path and the sense-of-shear can now be derived from the crystallographic fabric. Furthermore, it has been suggested that the fabric patterns can resolve the relative components of pure and simple shear in a deformation event (Dietrich & Song 1984, Wenk *et al.* 1987).

Schmid *et al.* (1987) determined several deformation regimes in their simple shear experiments. From lower to higher temperature these are: regime 1, twinning regime, dominated by *e*-twinning and lesser dislocation glide on *r*-planes; regime 2, intracrystalline slip regime, with slip on *r*-, *f*- and basal-planes; and regime 3, grain-boundary sliding regime. Wenk *et al.* (1987) determined two textural regimes in their Taylor simulations and experiments: a low-temperature regime, with *e*-twinning and *r*-slip active, and a high-temperature regime, with *r*- and *f*-slip, and *e*-twinning active. To a first order, regime 1 of Schmid *et al.* (1987) corresponds to the low-temperature textures of Wenk *et al.* (1987), and regime 2 corresponds to the high-temperature textures.

The low to moderate M_2 metamorphic temperatures (which did not exceed M_1 temperatures of 350–400°C) and the large grain size of the Guilmette marbles enhance *e*-twinning as a dominant deformation mechanism. In thin section, *e*-twins are well developed and weak undulose extinction and bent *e*-twins indicate that dislocation glide along *r*-planes was also active. The Guilmette marbles were deformed in the twinning regime, and therefore their crystallographic textures should correspond to the low-temperature textures of Wenk *et al.* (1987).

Symmetric *c*- and *a*-axis pole figures relative to the grain shape fabric are generally interpreted to develop during coaxial deformation (Wenk *et al.* 1973, 1987, Wagner *et al.* 1982). For simple shear deformation, an asymmetric orientation pattern is developed. In the simple shear experiments of Schmid *et al.* (1987) the macroscopic flattening fabric is not coincident with the shear plane, and the asymmetry is very subtle with respect to the flattening fabric (Schmid *et al.* 1987), but more pronounced with respect to the shear plane. However, published examples of natural calcite tectonites suggest that, most commonly, the shear planes are parallel to the macroscopic foliation (Schmid *et al.* 1981, Dietrich & Song 1984, Wenk *et al.* 1987). In the Guilmette marbles, the only shear planes in these rocks appear to post-date the flattening fabrics, and furthermore, they are parallel to the macroscopic foliation.

Dietrich & Song (1984) proposed that the angle between the *a*-axis girdle and the macroscopic foliation plane (assumed to be the shear plane) is related to the relative component of simple shear in the total deformation. This proposition is based on the observation that in simple shear deformation, the incremental stress and strain axes are oriented 45° to the shear plane (Ramsay 1980). They suggested that the *a*-axis girdle corresponds to the infinitesimal flattening plane, and that the macroscopic cleavage, at least for their study area, is parallel to the shear-zone boundary. The correspondence of the *a*-axis girdle to the incremental flattening plane is supported by: (1) experimental and theoretical results of coaxially deformed marbles, which yield broad *c*-axis concentrations around the compression axis (ideally distributed around a small circle, 26° from the

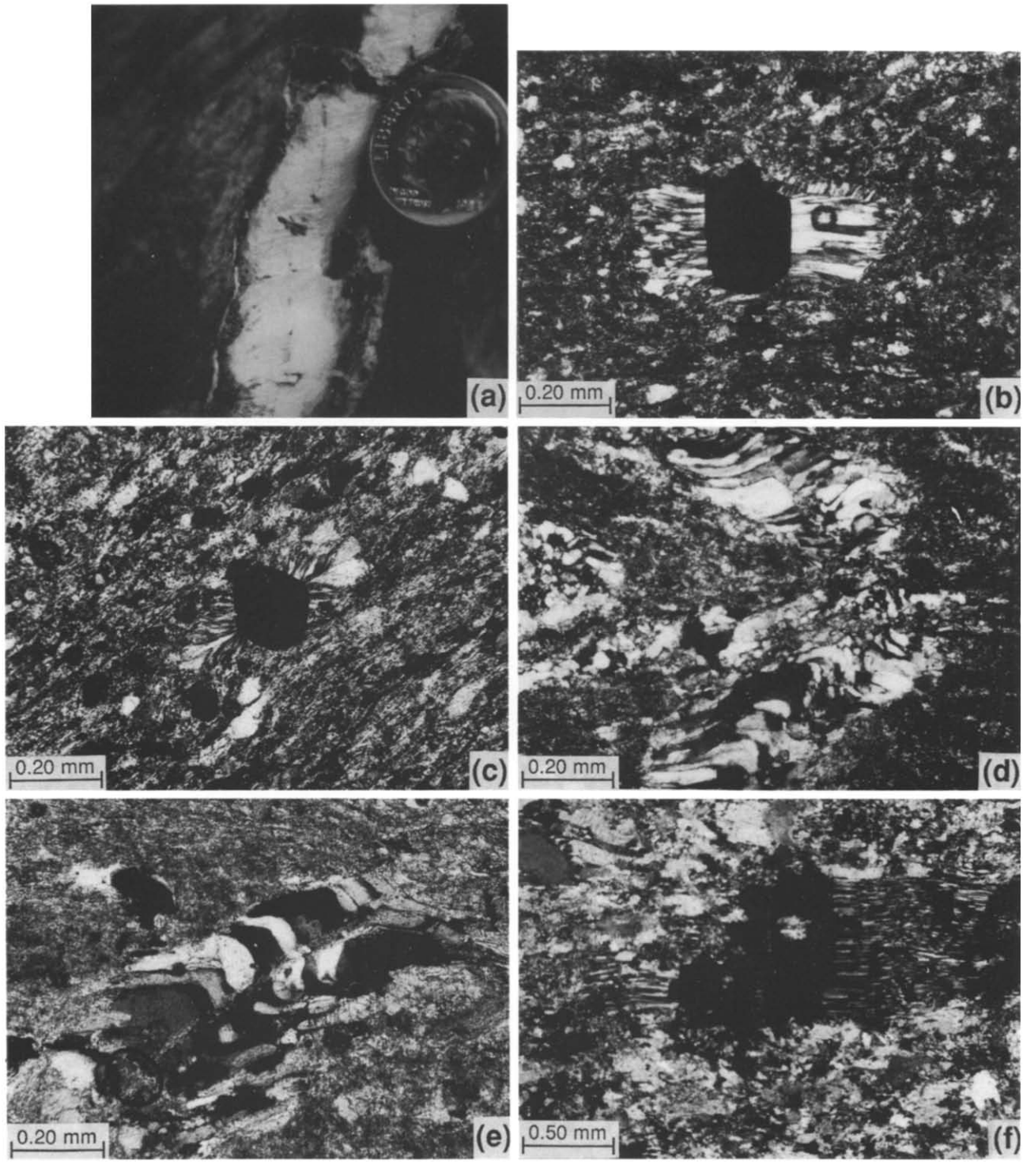

Fig. 9. Field photograph and photomicrographs of strain path indicators. (a) Close up of antitaxial calcite vein. Note the well-developed medial suture, and the parallelism between the fibers at the vein margin (last increment) and cleavage. (b) & (c) Coaxial, face-controlled pressure shadows around pyrite. The straight suture between quartz fibers originating from adjacent crystal faces indicates coaxial deformation. (d) & (e) Antitaxial quartz veins within Oquirrh limestone. (f) Fibrous quartz pressure shadow/pull-apart structure in chert-rich limestone.

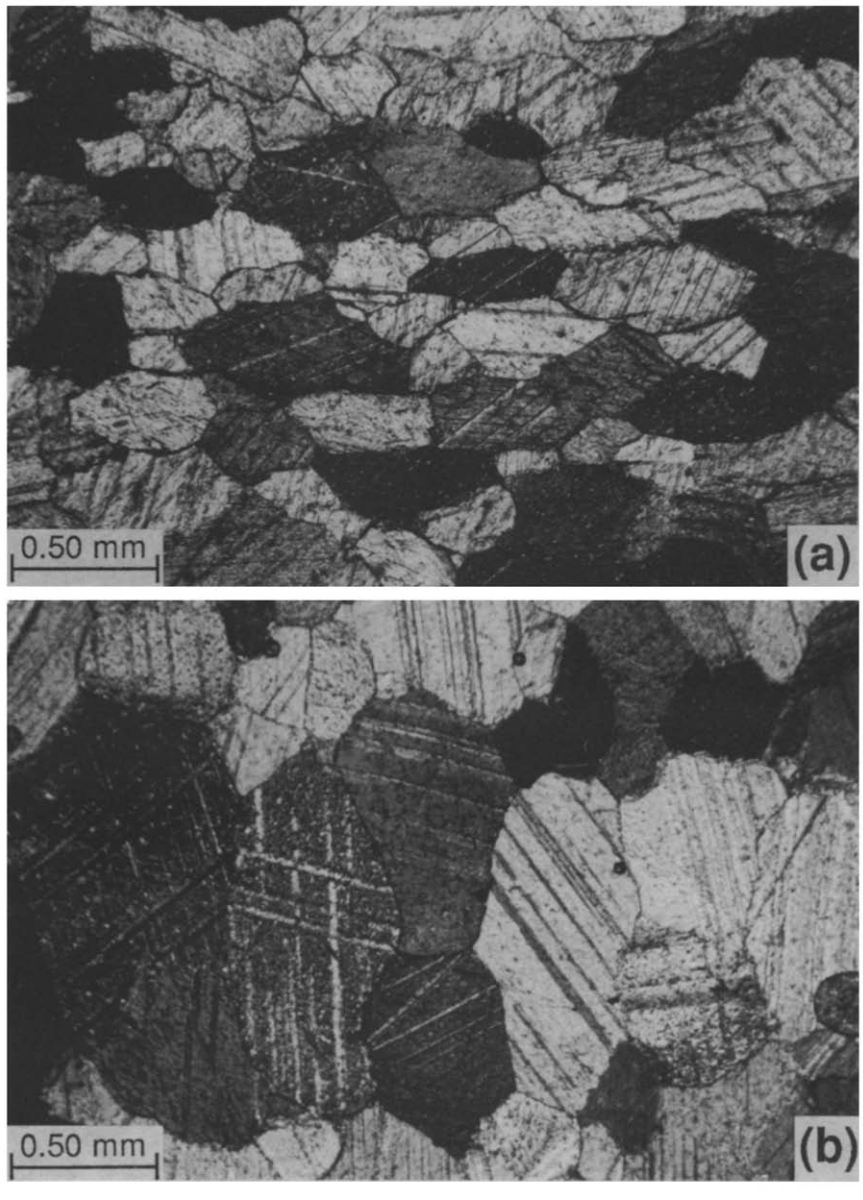

Fig. 10. Photomicrographs of the Guilmette limestone. (a) Microscopic foliation defined by elongate calcite grains. This fabric is parallel to the macroscopic cleavage. (b) Lineation within the foliation plane.

compression axis) (Turner *et al.* 1956, Wenk *et al.* 1973, 1987, Rutter & Rusbridge 1977, Wagner *et al.* 1982); and (2) natural examples exhibiting late stage matrix grains with a grain shape fabric oblique to the macroscopic foliation, where *c*-axis maxima are commonly perpendicular to the matrix grain shape fabric (Schmid *et al.* 1981, Dietrich & Song 1984). Wenk *et al.* (1987), using their Taylor calculations for the low-temperature regime, suggested that the displacement angle, ω, between the *c*-axis maxima and the normal to the macroscopic foliation plane (again assumed to be the shear plane) could be used to calculate the components of pure and simple shear in the overall deformation (note that the angle ω is equivalent to the angle between the *a*-axis girdle and the macroscopic foliation). The results of these two methods for determining the relative components of pure and simple shear, those of Dietrich & Song (1984) and those of Wenk *et al.* (1987), are very similar.

For the study of the Guilmette marbles, *c*-axes [0001] were measured on the universal stage in six samples. To allow comparison of these optically-derived *c*-axis pole figures with X-ray-derived pole figures that frequent the current literature, *a*-axis [$2\bar{1}\bar{1}0$] orientations were determined using X-ray pole figure goniometry on one sample, BP410 (using a Scintag PAD V X-ray system with a Huber pole figure goniometer at Cornell University). Combined reflection and transmission scans were used, with counting times of 50 s for each 5° step in tilt and azimuth and 100 s on two background positions for each tilt position. Crystallographically, the three *a*-axes define a plane whose pole is the *c*-axis. Therefore, on a pole figure, the pole to the girdle defined by *a*-axes will correspond to the *c*-axis maxima.

All samples of Guilmette marbles exhibit a strong preferred orientation of *c*- and *a*-axes (Figs. 11a–g). Samples BP74 and BP410 exhibit symmetric to slightly asymmetric fabrics relative to the foliation plane (Figs. 11b,c & g). Sample BP410 was measured both on the universal stage (Fig. 11c) and by X-ray analysis (Fig. 11g) and the results are very similar. *c*-axis maxima correspond to normals to the microscopic foliation (defined by calcite grain shape fabric), and *a*-axis girdles lie within the microscopic foliation plane. Based on the previous experimental and theoretical results described above, the symmetric patterns are interpreted to record coaxial deformation.

Samples BP202, BP206, BP205 and BP204 are slightly more asymmetric with respect to the foliation normal (obliquities between 6° and 8°). Using the methods of Dietrich & Song (1984) and Wenk *et al.* (1987), the component of pure shear recorded in the Guilmette marbles has been derived from the fabric obliquity, ω (Table 1). The pure shear component recorded in these textures is far greater than the component of simple shear, and ranges from 76 to 100%. Furthermore, the asymmetries of these samples are not all in the same direction, suggesting that different samples have minor components of simple shear strain but of opposite sense; an inconsistency that supports the interpretation of bulk coaxial deformation. A similar relationship of slightly asymmetric calcite fabrics (obliquity up to 10°), but with an inconsistent sense, was described by Erskine & Wenk (1985) from the Santa Rosa mylonite zone. Their samples are from a group that largely exhibit symmetric fabrics. Based on these calcite textures, Erskine & Wenk (1985) also concluded that the mylonite zone developed in pure shear.

Table 1

Sample	ω (°)	Pure shear (%)	Simple shear (%)
202	8	76	24
74	2	94	6
410	0	100	0
206	6	81	19
205	7	78	22
204	7	78	22

In summary, crystallographic fabrics from the Guilmette samples indicate that 76–100% of the total strain developed during pure shear. West-vergent simple shear zones are superimposed on this earlier fabric.

DISCUSSION

Lithologic control

It has been suggested that naturally deformed marbles partition pure shear deformation in preference to simple shear (Erskine & Wenk 1987). The majority of the fabrics described here are from carbonates, and this might explain the preferential development of pure shear textures. However, several observations suggest that the pure shear recorded in these rocks is not simply the result of lithologic control, but rather reflects a more general or bulk strain.

In the Black Pine Mountains, localities T1 and T2 occur within siltite interbeds within limestone. Either the strain path of the surrounding limestone imposes restricting boundary conditions on the enclosed siltite and essentially governs the strain path for this horizon, or quartz/clay-rich lithologies were independently deforming by a coaxial strain path (note that a variation in strain path between differing lithologies does require dislocation surfaces or high strain zones between these lithologies to maintain strain compatibility). In either event, however, other crystallographic fabrics from marbles indicate that the predominance of pure shear strain in marbles is not always the case.

Our preliminary work in the upper plate in the eastern Raft River Mountains as well as the work of Dietrich & Song (1984), suggests that carbonates can deform by large amounts of simple shear strain. Sample RR3B is a marble tectonite from the base of an allochthon in the eastern Raft River Mountains and it records a crystallographic fabric obliquity of 20° (Fig. 11h), corresponding to 60% simple shear. The marbles studied by Dietrich & Song (1984) record simple shear values between 35 and

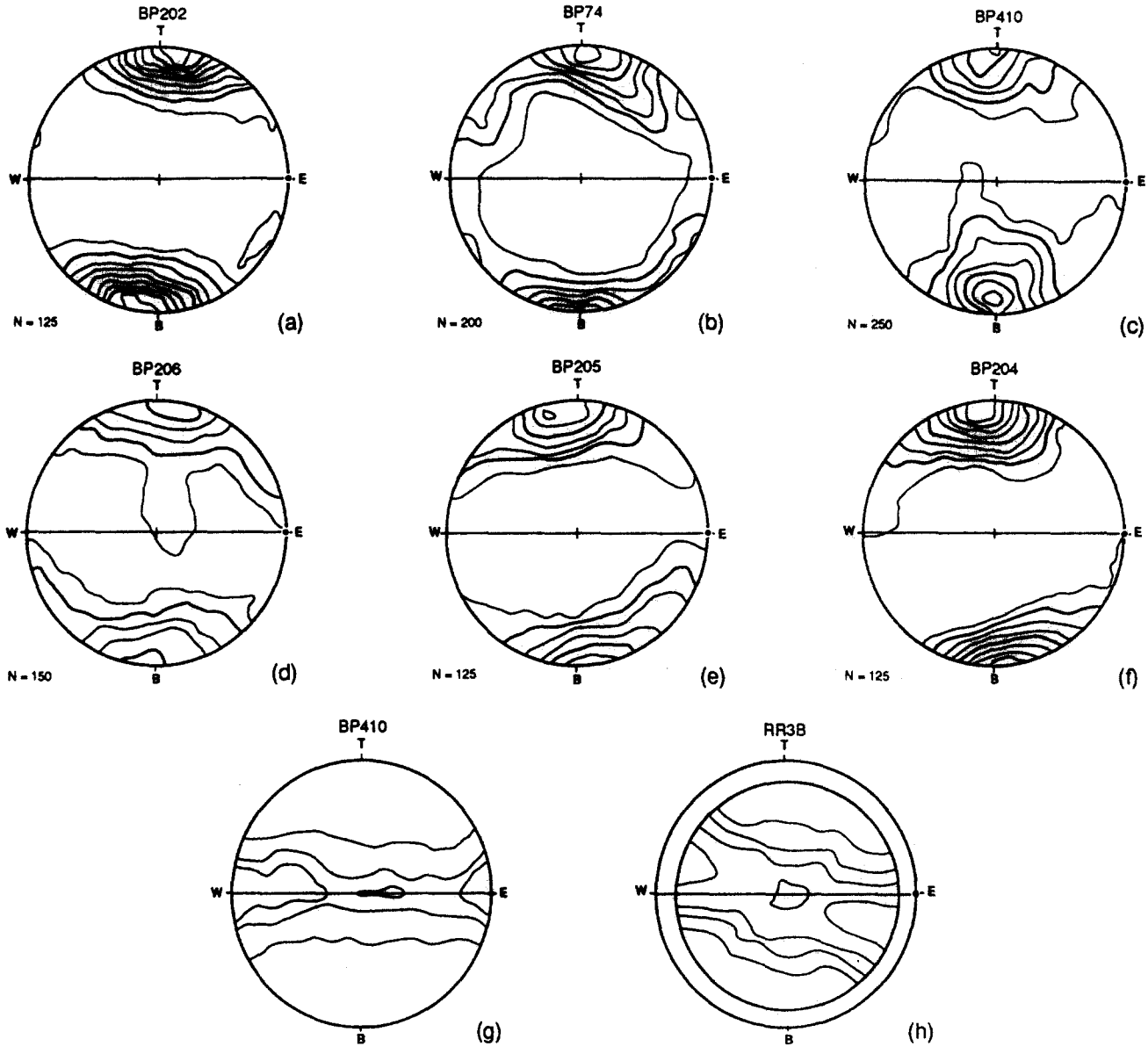

Fig. 11. Pole figures for deformed marbles. The E–W line represents the macroscopic cleavage plane (coincident with the microscopic foliation) and the lineation is indicated by the filled circle. (a)–(g) are from the Black Pine Mountains; (h) is from the eastern Raft River Mountains. (a)–(f) Optically measured *c*-axis pole figures from the Guilmette limestone. (b)–(d) are from two perpendicular thin sections (perpendicular to foliation and parallel to lineation and perpendicular to both foliation and lineation); (a), (e) & (f) are each measured from one section cut perpendicular to foliation and parallel to lineation. Contouring by the Kamb method, contours of 2, 4, 6, 8, 10, 12, 14, 16 and 18 sigma; 4, 10, 16 sigma are in bold. (g) & (h) X-ray derived *a*-axis pole figures. Contoured by 1% area, contours of 1%, 1.5%, 2.0% and 2.5% (equivalent to 1, 1.5, 2.0 and 2.5 of random distribution).

100%. These examples illustrate that marbles can deform by a large component of simple shear.

Quartzites within the lower plate of the eastern Raft River metamorphic core complex (15 km to the southwest of the Black Pine Mountains) locally exhibit coaxial fabrics (symmetric quartz *c*-axis crossed girdles, Compton 1980, Sabisky 1985, Malavieille 1987). Although correlation between these coaxial fabrics and those in the Black Pine Mountains cannot be made, these data illustrate that non-carbonate lithologies in the near-region locally record a large pure shear component. Possibly this event(s) is recorded at the structural level of the Black Pine Mountains, where the correlative pure shear component of penetrative elongation was dominant. In any case, we conclude that the pure shear deformation documented from the Black Pine Mountains is not an artifact of incomplete sampling of a restricted lithologic type, but rather reflects a more regional strain path.

Tectonic setting

The central intent of this paper is to document the strain and strain path for the Middle Paleozoic rocks within the Black Pine Mountains. However, these results are contrary to many previous studies in the region, and warrant a brief discussion of the possible tectonic settings in which this bedding-parallel elongation took place. Were these rocks elongated within a framework of regional upper crustal extension or shortening?

Throughout northwestern Utah, northeastern Nevada and southern Idaho, numerous occurrences of bedding-parallel attenuation have been documented (Compton *et al.* 1977, Miller 1980, Miller *et al.* 1987). It has been proposed that many of these structures are Mesozoic in age and developed during regional shortening (Snoke & Miller 1988). Based on the known finite strain and strain path, and probable deformation age, some constraints can be placed on the tectonic setting during which the bedding-parallel fabrics were developed.

Elongation parallel to sub-horizontal bedding can be produced within compressional allochthons, and generally occurs within shear zones that are sub-parallel to bedding. However, fabrics developed in this manner will have a significant non-coaxial component. This predominance of non-coaxial deformation in shear zones is well anchored in theoretical principles (Ramsay & Graham 1970, Ramsay 1980), and has been noted by many authors from many different mountain belts (i.e. see Law *et al.* 1984, p. 495). Exceptions, however, are the coaxial quartz *c*-axis fabrics reported by Law *et al.* (1984) from the Moine thrust zone. Law *et al.* (1984) interpreted these fabrics as representing a distinct coaxial domain, lying above a non-coaxial domain, both occurring within a single thrust sheet. Although the following distinction is obvious, we would like to emphasize that a domain of sub-horizontal elongation fabrics with a coaxial deformation history requires that these fabrics developed during sub-horizontal extension, not shortening. The distinct coaxial and non-coaxial kinematic domains of Law *et al.* (1984) represent kinematic domains of horizontal extension and horizontal shortening, respectively.

We interpret the coaxial fabrics within the Black Pine Mountains as representing a kinematic domain where elongation parallel to bedding was dominantly coaxial, and was developed during extension. However, the probable late Cretaceous ages for these fabrics suggest that they developed during a period of regional shortening in the fold and thrust belt to the east. Because foreland thrusts are known to cut down section and root in the hinterland to the west, shortening was occurring (in the late Cretaceous) at depth beneath the Black Pine Mountain strata. Therefore, the extension must have been restricted to the upper crust, requiring decoupling to accommodate crustal shortening at deeper structural levels. Law *et al.* (1984) proposed several tectonic settings for the development of coaxial extensional fabrics structurally above a non-coaxially deforming domain within a compressional orogen, including: (1) coaxial thinning in the hanging wall above a ramp; (2) coaxial thinning due to emplacement of an overlying culmination; (3) gravitational spreading produced by a thickened orogenic bulge. The available data do not allow us to unequivocally determine which of these models is applicable to the Black Pine Mountain fabrics. However, we suggest that a variation of model (3) is most plausible.

Several recent studies have noted that upper crustal extension within uplifted orogenic interiors can occur concurrently with shortening in the foreland. Horizontal extension has been documented in the Tibetan Plateau (Molnar & Chen 1983, Burchfiel & Royden 1985), and within the Puna-Altiplano Plateau in Bolivia and Argentina (Dalmayrac & Molnar 1981, Allmendinger 1986). Perhaps the contrasting late Cretaceous kinematic regimes of extension and shortening within the Sevier Belt hinterland (apparently simultaneously active at different crustal levels) represent an analogous situation to the examples cited above, where horizontal extension results from gravitational collapse triggered by topographic uplift and crustal thickening.

The earliest documented extension in the Sevier Belt hinterland is as much as 50 Ma younger than the late Cretaceous metamorphic ages from the Black Pine Mountains; in the Raft River–Grouse Creek–Albion metamorphic terrane, the earliest recorded extension is of late Eocene age (Saltzer & Hodges 1988). However, despite the large separation in time, striking similarities exist between extension directions recorded in the Raft River metamorphic core, the brittle high-angle faults within the upper plate of the Miocene and younger Raft River detachment, and the earlier layer-parallel fabrics occurring within the Black Pine Mountains.

The kinematics of brittle extension from 31 high-angle faults within the Paleozoic rocks of the Black Pine Mountains were determined, using the graphical methods of Allmendinger (1986). Best-fit representative kinematic axes were determined to be ESE–WNW extension and vertical shortening (Figs. 12a & b). This extension direction is very similar to the ~E–W least principal stress orientation determined by Malavielle (1987) for brittle faulting in upper plate Paleozoic rocks within the eastern Raft River Mountains. Stretching lineations from the footwall extensional shear zone in the eastern Raft River Mountains indicate ~E–W extension (Fig. 12b). These data are very similar to finite-strain extension directions determined by Compton (1980), Sabisky (1985) and Malavielle (1987), whose studies also indicated vertical shortening. Comparison of the extension and shortening directions recorded by the layer-parallel fabrics of Black Pine Mountains (Fig. 5), with extension and shortening directions for both the brittle and ductile extension associated with the Raft River detachment indicates that, although these events are widely separated in time, the orientation of kinematic axes are very similar. Perhaps the early episode of extension recorded in the Black Pine Mountains represents an early precursor event, resulting from a similar orogenic architecture that led to the widespread Cenozoic extension recorded in the core complexes.

The coaxial fabrics discussed above from the Black Pine Mountains are one of only several documentations (Lee *et al.* 1987) of coaxial layer-parallel elongation developed during extension. We emphasize that these fabrics are older than common Tertiary extension in the Great Basin, and presently occur in the upper plate of a prominent core complex detachment fault. Because the pre-Tertiary structural setting in which these fabrics developed is poorly known, they are difficult to place

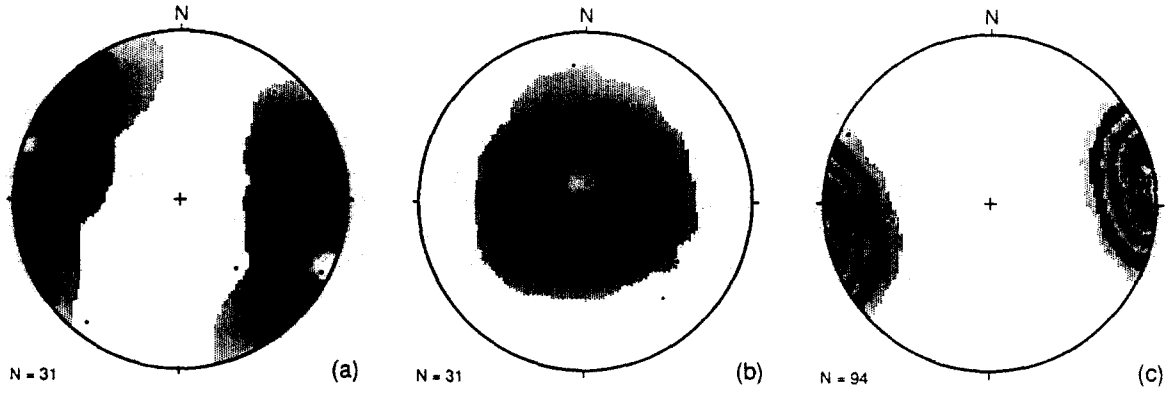

Fig. 12. (a) & (b) Kinematics of high-angle normal faults in the Black Pine Mountains. Data are plotted as lower-hemisphere, equal-area stereographic projections, contouring is by the Kamb method; contours of 2, 4, 6, 8 and 10 sigma. (a) Extension axes, (b) shortening axes and (c) stretching lineations from the mylonitic parautochthon in the eastern Raft River Mountains.

within a geometric framework of crustal extension. Although we do not advocate wholesale ductile necking of the crust, the mere existence of these fabrics alone suggests that coaxial deformation might locally be a dominant strain path during extension. Possible structural settings for coaxial deformation during extension are deforming interiors of shear-zone-bounded lenses or megaboudins (Davis 1980, Hamilton 1987).

CONCLUSIONS

Paleozoic rocks exposed within the Black Pine Mountains have undergone a complex, yet decipherable structural history. Geologic mapping and strain analysis suggest that the earliest recorded event is an E–W bedding-parallel extension of 160%. Incremental strain and petrofabric data suggest that the attenuation fabrics were developed during a progressive pure shear deformation. The occurrence of these coaxial fabrics outside extensional shear zones exposed in core complexes, and in lesser strained rocks, suggests that pure shear might locally be an important component in the attenuation of rocks, and that pure shear fabrics can be easily obscured.

Although widespread extension in the Sevier Belt hinterland began in the middle Cenozoic, preliminary geochronology suggests a late Cretaceous age for the early extension in the Black Pine Mountains. Extension of the Black Pine Mountain strata was probably occurring synchronously with shortening at deeper crustal levels, and could possibly be caused by gravitational collapse of a thickened and topographically elevated crust. Further geochronological and structural studies in the Sevier Belt hinterland need to address the deformation of rocks not affected by Tertiary strain and metamorphism to further evaluate the extent of this late Cretaceous(?) extensional deformation.

Acknowledgements—We thank D. Sarewitz, T. Jordan and J. Hibbard, for their thoughtful suggestions and criticisms of earlier versions of this work. Additionally, we thank an anonymous reviewer for helpful comments and suggestions for improving this manuscript. We have benefited from discussions with D. Miller, D. Harding and T. Heyn. The field work was made possible by funding provided by Amoco Production Company, Chevron U.S.A. Inc., the Geological Society of America, the American Association of Petroleum Geologists, and Sigma XI. Funding provided by National Science Foundation Grant EAR-8720952 supported the laboratory-based analyses.

REFERENCES

Allmendinger, R. W. 1986. Tectonic development, southeast border of the Puna Plateau, northwest Argentine Andes. *Bull. geol. Soc. Am.* **97**, 1070–1082.

Allmendinger, R. W. & Jordan, T. E. 1984. Mesozoic structure of the Newfoundland Mountains, Utah: horizontal shortening and subsequent extension in the hinterland of the Sevier orogenic belt. *Bull. geol. Soc. Am.* **95**, 1280–1292.

Allmendinger, R. W., Miller, D. M. & Jordan, T. E. 1984. Known and inferred Mesozoic deformation in the hinterland of the Sevier orogenic belt, northwest Utah. *Utah Geol. Ass. Publ.* **13**, 21–34.

Armstrong, R. L. 1976. The geochronometry of Idaho. *Isochron/West* **15**, 1–33.

Burchfiel, B. C. & Royden, L. H. 1985. North-south extension within the convergent Himalayan region. *Geology* **13**, 679–682.

Burg, J. P. & Harris, L. B. 1982. Tension fractures and boudinage oblique to the maximum extension direction: An analogy with Luders bands. *Tectonics* **83**, 347–363.

Casey, M., Rutter, E. H., Schmid, S. M., Siddans, A. W. B. & Whalley, J. S. 1978. Texture development in experimentally deformed calcite rocks. In: *Proc. 5th Int. Conf. on Textures of Materials*. Springer, Berlin, 231–240.

Compton, R. R. 1980. Fabrics and strains in quartzites of a metamorphic core complex, Raft River Mountains, Utah. In: *Cordilleran Metamorphic Core Complexes* (edited by Crittenden, M. D., Jr, Coney, P. J. & Davis, G. H.). *Mem. geol. Soc. Am.* **153**, 385–398.

Compton, R. R., Todd, V. R., Zartman, R. E. & Naeser, C. W. 1977. Oligocene and Miocene metamorphism, folding, and low-angle faulting in northwestern Utah. *Bull. geol. Soc. Am.* **88**, 1237–1250.

Covington, H. R. 1983. Structural evolution of the Raft River Basin, Idaho. In: *Tectonic and Stratigraphic Studies in the Eastern Great Basin* (edited by Miller, D. M., Todd, V. R. & Howard, K. A.). *Mem. geol. Soc. Am.* **157**, 229–237.

Crittenden, M. D., Jr, Coney, P. J. & Davis, G. H. (editors) 1980. Cordilleran Metamorphic Core Complexes. *Mem. geol. Soc. Am.* **153**, 490.

Dallmeyer, R. D., Snoke, A. W. & McKee, E. H. 1986. The Mesozoic–Cenozoic tectonothermal evolution of the Ruby Mountains, east Humboldt Range, Nevada: a Cordilleran Metamorphic Core Complex. *Tectonophysics* **5**, 931–954.

Dalmayrac, B. & Molnar, P. 1981. Parallel thrust and normal faulting in Peru and constraints on the state of stress. *Earth Planet. Sci. Lett.* **55**, 473–481.

Davis, G. H. 1980. Structural characteristics of metamorphic core complexes, southern Arizona. In: *Cordilleran Metamorphic Core Complexes* (edited by Crittenden, M. D., Jr, Coney, P. J. & Davis, G. H.). *Mem. geol. Soc. Am.* **153**, 35–77.

Davis, G. H. 1983. Shear-zone model for the origin of metamorphic core complexes. *Geology* **13**, 342–347.

DeWitt, E. 1980. Comment on "Geologic development of the Cordilleran metamorphic core complexes". *Geology* **8**, 6–9.
Dietrich, D. & Song, H. 1984. Calcite fabrics in a natural shear environment; Helvetic nappes of western Switzerland. *J. Struct. Geol.* **6**, 19–32.
Doelling, H. 1980. Geology and Mineral resources of Box Elder County, Utah. *Bull. Utah Geol. Miner. Surv.* **115**, 251.
Durney, D. W. & Ramsay, J. G. 1973. Incremental strains measures by syntectonic crystal growths. In: *Gravity and Tectonics* (edited by De Jong, K. A. & Scholten, R.). Wiley, New York, 67–96.
Erskine, B. G. & Wenk, H.-R. 1985. Evidence for late Cretaceous crustal thinning in the Santa Rosa mylonite zone, southern California. *Geology* **13**, 274–277.
Erskine, B. G. & Wenk, H.-R. 1987. Calcite lattice preferred orientation and microstructures in deformed Cordilleran marbles: Correlation of shear indicators and determination of strain path. *Geol. Soc. Am. Abs. w. Prog.* **19**, 656.
Flinn, D. 1962. On folding during three-dimensional progressive deformation. *Q. J. geol. Soc. Lond.* **118**, 385–433.
Gaudemer, Y. & Tapponnier, P. 1987. Ductile and brittle deformations in the northern Snake Range, Nevada. *J. Struct. Geol.* **9**, 159–180.
Goldstein, A. G. 1988. Factors affecting the kinematic interpretation of asymmetric boudinage in shear zones. *J. Struct. Geol.* **10**, 707–716.
Hamilton, W. 1987. Crustal extension in the Basin and Range Province, southwestern United States. *Spec. Publs J. geol. Soc. Lond. Continental Extensional Tectonics* **28**, 155–176.
Hanmer, S. 1986. Asymmetrical pull-aparts and foliation fish as kinematic indicators. *J. Struct. Geol.* **8**, 111–122.
Kern, H. & Wenk, H.-R. 1983. Texture development in experimentally induced ductile shear zones. *Contr. Miner. Petrol.* **83**, 231–236.
Law, R. D., Knipe, R. J. & Dayan, H. 1984. Strain partitioning within thrust sheets: microstructural and petrofabric evidence from the Moine Thrust zone at Loch Eriboll, northwest Scotland. *J. Struct. Geol.* **6**, 477–497.
Lee, J., Miller, E. L. & Sutter, J. F. 1987. Ductile strain and metamorphism in an extensional tectonic setting—a case study from the northern Snake Range, Nevada, U.S.A. *Spec. Publs J. geol. Soc. Lond. Continental Extensional Tectonics* **28**, 267–298.
Lister, G. S. & Snoke, A. W. 1984. S–C mylonites. *J. Struct. Geol.* **1**, 99–115.
Malavieille, J. 1987. Extensional shearing deformation and kilometer-scale "a" type folds in a Cordilleran metamorphic core complex (Raft River Mountains, northwestern Utah). *Tectonics* **6**, 423–448.
Miller, D. M. 1980. Structural geology of the northern Albion Mountains, south-central Idaho. In: *Cordilleran Metamorphic Core Complexes* (edited by Crittenden, M. D., Jr, Coney, P. J. & Davis, G. H.). *Mem. geol. Soc. Am.* **153**, 399–423.
Miller, D. M., Hillhouse, W. C., Lanphere, M. A. & Zartman, R. E. 1987. Geochronology of intrusive and metamorphic rocks in the Pilot Range, Utah and Nevada, and comparison with regional patterns. *Bull. geol. Soc. Am.* **99**, 866–879.
Miller, D. M., Wooden, J. L. & Wright, J. E. 1989. Mantle-derived Late Jurassic plutons emplaced during possible regional extension of the crust, northwest Utah and northeast Nevada (abs). *Geol. Soc. Am. Abs. w. Prog.* **21**, 116.
Miller, E. L. & Gans, P. B. 1989. Cretaceous crustal structure and metamorphism in the hinterland of the Sevier thrust belt, western U.S. Cordillera. *Geology* **17**, 59–62.
Miller, E. L., Gans, P. B. & Garing, J. 1983. The Snake Range decollement: an exhumed mid-Tertiary ductile–brittle transition. *Tectonics* **2**, 239–263.
Miller, E. L., Gans, P. B., Wright, J. E. & Sutter, J. F. 1988. Metamorphic history of the east central Basin and Range province: tectonic setting and relationship to magmatism. In: *Metamorphism and Crustal Evolution of the Western United States, Rubey Volume VII* (edited by Ernst, W. G.). Prentice-Hall, Englewood Cliffs, New Jersey, 649–682.
Molnar, P. & Chen, W.-P. 1983. Focal depths and fault plane solutions of earthquakes under the Tibetan plateau. *J. geophys. Res.* **88**, 1180–1096.
Oriel, S. S., Williams, P. L., Covington, H. R., Keys, W. S. & Shaver, K. C. 1978. Deep drilling data, Raft River Geothermal area, Idaho; Standard American Oil Company Malta, Naf and Strevell petroleum test boreholes. *U.S. geol. Surv. Open-File Rep.* **78-361**.
Ramberg, H. 1959. Evolution of ptygmatic folding. *Norsk geol. Tidsskr.* **39**, 99–152.
Ramsay, J. G. 1980. Shear zone geometry: a review. *J. Struct. Geol.* **2**, 83–99.
Ramsay, J. G. & Graham, R. H. 1970. Strain variation in shear belts. *Can. J. Earth Sci.* **7**, 786–813.
Ramsay, J. G. & Huber, M. I. 1983. *The Techniques of Modern Structural Geology. Volume* 1: *Strain Analysis.* Academic Press, New York, 307.
Rehrig, W. A. & Reynolds, S. J. 1980. Geologic and geochronologic reconnaissance of a northwest-trending zone of metamorphic core complexes. In: *Cordilleran Metamorphic Core Complexes* (edited by Crittenden, M. D., Jr, Coney, P. J. & Davis, G. H.). *Mem. geol. Soc. Am.* **153**, 131–157.
Rutter, E. H. & Rusbridge, M. 1977. The effect of non-coaxial strain paths on crystallographic preferred orientation development in the experimental deformation of marble. *Tectonophysics* **39**, 73–86.
Sabisky, M. A. 1985. Finite strain, ductile flow, and folding in the central Raft River Mountains, northwestern Utah. Unpublished M.S. thesis, University of Utah.
Saltzer, S. D. & Hodges, K. V. 1988. The Middle Mountain shear zone, southern Idaho: kinematic analysis of an early Tertiary high-temperature detachment. *Bull. geol. Soc. Am.* **100**, 96–103.
Sanderson, D. J. 1974. Patterns of boudinage and apparent stretching lineation developed in folded rock. *J. Geol.* **82**, 651–661.
Schmid, S. M., Casey, J. & Starkey, J. 1981. The microfabric of calcite tectonites from the Helvetic nappes (Swiss Alps). In: *Thrust and Nappe Tectonics* (edited by McClay, K. & Price, N. J.). *Spec. Publs geol. Soc. Lond.* **9**, 151–158.
Schmid, S. M., Panozzo, R. & Bauer, S. 1987. Simple shear experiments on calcite rocks: rheology and microfabric. *J. Struct. Geol.* **9**, 747–778.
Smith, J. F. 1982. Geologic Map of the Strevell 15 minute quadrangle, Cassia County, Idaho. *U.S. geol. Surv.* Map I-1403.
Smith, J. F. 1983. Paleozoic rocks in the Black Pine Mountains, Cassia County, Idaho. *Bull. U.S. geol. Surv.* **1536**, 36.
Snoke, A. W. & Miller, D. M. 1988. Metamorphic and tectonic history of the northeastern Great Basin. In: *Metamorphism and Crustal Evolution of the Western United States. Rubey Volume VII* (edited by Ernst, W. G.). Prentice-Hall, Englewood Cliffs, New Jersey, 606–648.
Turner, F. J. & Ch'ih, C. S. 1951. Deformation of Yule marble, Part III. Observed fabric changes due to deformation at 10,000 atmospheres confining pressure, room temperature, dry. *Bull. geol. Soc. Am.* **62**, 887–906.
Turner, F. J., Griggs, D. T., Clark, R. H. & Dixon, R. 1956. Deformation of Yule marble, Part VII. Development of oriented fabrics at 300 to 500°C. *Bull. geol. Soc. Am.* **67**, 1259–1294.
Turner, F. J. & Weiss, L. E. 1963. *Structural Analysis of Metamorphic Tectonites.* McGraw-Hill, New York, 545.
Wagner, F., Wenk, H. R., Kern, H., Van Houtte, P. & Esling, C. 1982. Development of preferred orientation in plane strain deformed limestone. Experiment and theory. *Contr. Miner. Petrol.* **80**, 132–139.
Wells, M. L. 1988. Structural geometry, sequence, and kinematics of the Black Pine Mountains, southern Idaho: implications from the cover rocks to metamorphic core complexes. Unpublished M.S. thesis, Cornell University.
Wells, M. L. & Allmendinger, R. W. 1987. Superposition of pure and simple shear in the cover rocks of metamorphic core complexes: the Black Pine Mountains, southern Idaho. *Geol. Soc. Am. Abs. w. Prog.* **19**, 887.
Wells, M. L., Dallmeyer, R. D. & Allmendinger, R. W. 1989. Sequential Mesozoic thermal events in upper plate rocks of the Raft River core complex, northwest Utah and southern Idaho. *Geol. Soc. Am. Abs. w. Prog.* **21**, 157.
Wenk, H.-R., Takeshita, T., Bechler, E., Erskine, B. G. & Matthies, S. 1987. Pure and simple shear calcite textures. Comparison of experimental, theoretical and natural data. *J. Struct. Geol.* **9**, 731–745.
Wenk, H.-R., Venkitasubramanyan, C. S. & Baker, D. W. 1973. Preferred orientation in experimentally deformed limestones. *Contr. Miner. Petrol.* **38**, 81–114.
Wernicke, B. 1981. Low-angle normal faults in the Basin and Range Province: nappe tectonics in an extending orogen. *Nature* **291**, 645–648.